Evaluation of Modeling Strategies for Seismic Analysis of Confined Masonry Structures

Bonisha Borah
Indian Institute of Technology Guwahati
Hemant B Kaushik (hemantbk@gmail.com)
Indian Institute of Technology Guwahati https://orcid.org/0000-0001-5896-6543
Vaibhav Singhal
Indian Institute of Technology Patna

Research Article

Keywords: Confined masonry, Nonlinear analysis, Wide-column model, Strut-and-tie model, Equivalent strut model, V-D strut model

Posted Date: April 5th, 2022

DOI: https://doi.org/10.21203/rs.3.rs-1506811/v1

Abstract

Numerical models are effective tools for nonlinear seismic analysis required for performance-based design of structures. However, their potential often falls short while simulating the behavior of masonry structures because of their complex anisotropic behavior. The complexity increases further for confined masonry (CM) where, in addition to masonry, RC confining members are constructed around the periphery of masonry walls such that the structure work in unison. Though some modeling schemes have been developed for linear and nonlinear analysis of CM walls, their applicability and accuracy are a matter of contention as they were based on different assumptions and theories. Most design codes do not specify modeling schemes due to limited research, especially considering the highly variable masonry properties. The limited modeling choices, some of which have not been validated sufficiently, pose difficulty for practicing engineers and limit their confidence in adopting them. The present work provides an understanding of the challenges on using different modeling strategies from an engineering practice perspective. Commonly adopted models were first used to simulate previously tested single-story CM wall specimens having different aspect ratios. The comparative assessment showed the efficacy of some schemes, while exhibiting ineffectiveness of others. The applicability of different methods was then assessed by analyzing a three-story CM building. The observed behavior clarified the characteristics and potentialities of different procedures, and provides direction to adopt better approaches for nonlinear analysis of CM walls.

1. Introduction

Confined masonry (CM) is a riveting building construction choice due to its economic viability for safe construction in seismic regions. This building typology has been practiced both in the form of non-engineered and engineered construction from single-story houses to six-story apartment buildings in several parts of the world, and is currently evolving as a popular construction technique in many other regions. Masonry walls, which are the primary load-resisting members in CM buildings, are constructed prior to the casting of small-sized reinforced concrete (RC) columns and beams known as tie-elements. The construction methodology improves the interface connection between the masonry walls and the tie-elements as the concrete is cast-in-place resulting in an integral composite action of the RC and the masonry elements, in addition to the reduction in the formwork cost (Borah et al. 2019, 2021a). The tie-elements confine the masonry walls to engage them under gravity as well as lateral loads for enhanced deformation capacity and better connectivity with the other walls and floor diaphragms.

The performance of CM buildings has been very satisfactory in past earthquakes (e.g., 2010 Maule, Chile earthquake (M 8.8), 2007 Pisco, Peru earthquake (M 8.0), 2005 Northern Sumatra, Indonesia earthquake (M 8.7), 2003 Bam, Iran earthquake (M 6.6), 2001 Offshore El Salvador earthquake (M 7.7), etc.). The reported failure modes in CM structures start with the shear-induced in-plane damages in the form of bed joint sliding or diagonal shear cracking emanating from the center of masonry wall and propagating towards the tie-columns. Further, it was observed that most low-rise CM houses did not experience any damage in earthquakes even with minor design flaws; however, a few CM buildings suffered severe damage, especially the mid-rise buildings (Galvis et al. 2020, Borah et al. 2019, Marques and Lourenço 2019, Brzev and Mitra 2018, Brzev 2007). The damage reports indicate some gaps still exist at the analysis and design levels that have to be addressed for safe and affordable design of CM buildings. Clearly, in order to proceed with seismic analysis and subsequent safer design, practical approaches for numerical modeling of CM buildings are needed to be investigated to capture the key behavioral features of CM buildings and to estimate accurate design forces under different loadings. Commonly adopted modeling strategies for CM walls are: wide column model (WCM), strut and tie model (STM), equivalent strut/shell model (ESM), and VD strut model (VDSM). Some of these methods were originally developed only for carrying out approximate linear analysis, while some were directly adopted from other building typologies. Considering the requirement of nonlinear analysis in performance based seismic design, some of the available methods have been modified to include the influence of material nonlinearity. The next section briefly provides

additional details of commonly adopted modeling strategies for CM walls. A comparative study of these modeling methods is essential to assess the effectiveness and limitations of the methods for simulating the lateral load behavior of 2-D CM walls as well as 3-D CM buildings. The present study is an attempt towards filling in some of these gaps in the seismic analysis of CM structures.

2. Review Of Modeling Strategies

Though CM building typology started after the 1908 Messina, Italy earthquake and exhibited many phenomenal performances in past seismic events; its engineering behavior has been established at a slow rate, and continues today. This is due to huge variation in materials and construction methodologies resulting in a limited understanding of the complex composite behavior under different loading conditions. Several empirical methods have been developed for approximately predicting the lateral capacity or backbone profile of CM walls as discussed in Borah et al. (2022). Further, limited studies have attempted some numerical modeling strategies for the analysis of CM buildings. This section provides a brief discussion on all the modeling strategies commonly adopted for CM walls as shown in Fig. 1. The strategies work at different degrees of refinement and precision, and can be preliminarily classified into two categories: (a) those using full 3D finite element (FE) models, and (b) those using simplified line element models.

The FE modeling technique is quite commonly used for numerical simulation of any complex structure to thoroughly study its behavior. A full 3D FE model of a CM wall comprises details of reinforcing bars, concrete tie-elements, and masonry wall with the provision of complete material nonlinearity and discretization using 3D finite elements (Fig. 1a). The masonry wall is modeled through different degrees of accuracy, e.g., (i) the sophisticated micro-modeling approach in which every component is modeled separately and defined by its individual nonlinear constitutive models, and (ii) macro-modeling approach in which masonry is defined as homogeneous material with isotropic or anisotropic laws. The micro modeling has also been done using a simplified approach in which bricks are expanded up to half of the mortar thickness in vertical and horizontal directions, and the mortar is clamped into mortar interface. Micro-modeling FE approaches are most suited for small structural elements in order to closely represent the heterogeneous states of masonry; and studies, such as Smoljanović et al. (2017) and Amouzadeh Tabrizi and Soltani (2017) utilized these approaches for CM. Whereas, macro-modeling FE approaches are used to represent the global structural behavior of masonry in CM wall as observed by Borah et al. (2021b and c, 2020), Marques et al. (2020), Yacila et al. (2019), Okail et al. (2016), Janaraj and Dhanasekar (2014), and Medeiros et al. (2013). However, the practical applicability of realistic and reliable FE models is very limited, especially for large structures, as they are computationally intensive, complex, and require a large number of input parameters that are not available easily.

In simplified 2D line element models, the elements of the building are modeled either as two-noded beam-column elements or as four-noded shell elements. Various popular simplified models developed in past literature are: wide-column model (WCM) (Rangwani and Brzev 2017, Terán-Gilmore et al. 2009, NTC-M 2004), strut-and-tie model (STM) (Rankawat et al. 2021, Tripathy and Singhal 2019, Ghaisas et al. 2017, Brzev and Gavilán 2016), equivalent strut/shell model (ESM) (Chakra-Varthy and Basu 2021, Borah et al. 2021b, Torrisi and Crisafulli 2017, Torrisi et al. 2012, and Kaushik and Sanganee 2010), and VD strut model (VDSM) (Borah et al. 2021b). As the present study is concerned about the practical applicability of the modeling strategies, a detailed evaluation of only these simplified models will be carried out in the following section.

2.1. Wide-Column Model (WCM)

Wide Column Model (WCM) for CM wall was mainly developed using the concept of equivalent frame model of unreinforced masonry (URM) wall structures (Kappos et al. 2002, Lagomarsino et al. 2013). Here, the masonry wall including the tie-columns is modeled as a one-dimensional two-noded centerline beam-column element (*wide* column) as

shown in Fig. 1b, with transformed section properties accounting for composite action of masonry and RC tie-columns. Thus, the width of tie-columns (w_{tc}) are transformed to equivalent masonry width so that the equivalent area of the wide column section (A_{wc}) is equal to:

$$A_{wc} = A_w + 2mA_c$$

1

where, A_w and A_c are the cross-sectional area of masonry wall and RC tie-column, respectively, and m is the modular ratio, i.e., the ratio of modulus of elasticity of concrete (E_c) to modulus of elasticity of masonry (E_m). Tie-beam is modeled using a two-noded beam-column element and the axial rigidity provided by the masonry wall below the tie-beams is simulated by modeling the tie-beam as rigid having an infinite stiffness because the connectivity between the tie-beam and the wide-column is realized through only a node. WCM has been recognized as a viable model (NTC-M 2004) as this technique provides the opportunity for the structural analysis of CM structure with commercial computer programs. Application of WCM for CM wall was demonstrated by Terán-Gilmore et al. (2009) by analyzing a three-story building where nonlinearity (axial lumped hinge) was defined near the bottom of each wide-columns using shear force-deformation relationship from a past empirical backbone model of CM wall. Further, Ranjbaran et al. (2012), Ahmad et al. (2012), and Rangwani and Brzev (2017) also demonstrated the applicability of WCM in analysis of CM structures.

2.2. Strut-and-Tie Model (STM)

STM was originally developed as a hand calculation procedure for the analysis and design of shear critical structures and D (disturbed) regions in concrete structures. In STM, based on experience and intuition, internal load paths are drawn through the structure in the form of trusses; i.e., compressive stress fields (represented by struts) are interconnected by tensile stress fields (represented by ties) and design member force resultants are computed using static equilibrium, provided the STM is statically determinate (Schlaich et al. 1987, Wight and MacGregor 2005). Considering the wall-type structures as analogous to very deep beams, where the entire wall represents the D region as per St. Venant's Principle, many past studies adopted STM. Considering that, STM analysis for CM walls subjected to lateral loading, i.e., pin-jointed structural truss connected by both tension and compression members (Fig. 1c), was suggested by NTC-M (2004), Brzev et al. (2007), Meli et al. (2011), etc. Horizontal component of diagonal strut force is used to determine the shear capacity of masonry wall. Whereas, the calculated tie forces are used to find the required amount of reinforcement in tie-members.

Brzev and Gavilán (2016) demonstrated the application of STM through a four-story two-bay CM wall, where one bay comprises of wall with opening in each story. The strut action of the walls with opening was disregarded in the study and the structure was analyzed for the given story shear forces. Ghaisas et al. (2017) showed that the orientation of strut elements is influenced by the openings and panel configurations, but the suggested configurations were not validated further for their ability to predict lateral capacity as well as load distribution in different members. To evaluate the lateral shear capacity of CM walls, Tripathy and Singhal (2019) proposed an empirical formula for the limiting axial capacity (F_{ss}) of diagonal strut in STM as:

$$F_{ss} = F_1\left(\sqrt{f'_m}A_w\right)$$

2

where, $F_1 = C_1\left(\frac{1}{\lambda}\right)\left(\frac{H}{L}\right) + C_2$ (3)

$$\lambda = H\left(\frac{E_m t \sin 2\theta}{4E_c I_c H}\right)^{0.25}$$

4

Here, for $H/L > 1$, $C_1 = 2.23$ and $C_2 = 0.1$; for $H/L \leq 1$, $C_1 = 2.65$ and $C_2 = 0.08$; $f_m^{'}$ is the compressive strength of masonry prism; A_w is the cross-sectional area of wall excluding tie-columns; H is the height of CM wall including the depth of tie-beam; L is the length of CM wall including the width of tie-columns; t is the wall thickness; I_c is the moment of inertia of tie-column section; θ is the angle between the strut centerline and the horizontal axis. The study suggested to consider the axial forces in ties by assuming the yielding of longitudinal reinforcement in tie-columns, i.e., $f_{yl}A_{sl}$, where A_{sl} is the total area of longitudinal reinforcing steel placed in a tie-column and f_{yl} is the yield strength of the rebar. Using this force in tie, axial force in the diagonal strut can be calculated using the method of joint (i.e., $f_{yl}A_{sl} / sin\theta$). If this force exceeds the limiting capacity (F_{ss}), then the axial force in strut is set to F_{ss} and the horizontal component of this force is treated as the lateral capacity of the wall. Rankawat et al. (2021) recently updated STM for CM walls such that it can be implemented in commercial software, and the method was renamed as Equivalent Truss Model. Using the relationship between lateral stiffness of wall (K_i) and axial stiffness of diagonal strut, the study suggested the width of the diagonal strut in STM as:

$$w_{ds} = \frac{K_i D^3}{tE_m L_c^2}$$

5

where, D is the length of the diagonal strut, L_c is the centerline length of CM wall in STM, K_i is the initial stiffness of wall that can be obtained considering the flexural and shear deformations of wall:

$$K_i = \left(\frac{H^3}{\beta E_m I} + \frac{\kappa H}{G_m A}\right)^{-1}$$

6

where, I is the moment of inertia of wall considering transformed section, $\kappa = 1.2$, $\beta = 3$ for cantilever, 12 for fixed ended wall. Further, applicability of the proposed model in nonlinear analysis was demonstrated on a three-story building where nonlinearity was defined only in the diagonal struts at the mid-section using the stress-strain relationships described in past empirical backbone model of CM walls.

2.3. Equivalent Strut/Shell Model (ESM)

Equivalent Strut Model (Fig. 1d) was originally developed for simulating the lateral load behavior of masonry infill walls in framed structures (Polyakov 1956, Holmes 1961, Stafford-Smith 1962). It gained much popularity because of simplicity and requirement of limited computational efforts. The simplest ESM include a single pin-jointed diagonal strut connected between the beam-column joints. The width of diagonal strut was suggested to be taken as one-third of the diagonal length of infill walls (Holmes 1961). However, later it was found that this model overestimates the actual stiffness of infilled frame. Therefore, based on different experimental and analytical observations, the effective width was defined through different empirical formulations. A commonly adopted generalized form of the effective width has been one-fourth of the diagonal length of infill frames (Paulay and Priestley 1992). It has been argued that a single diagonal strut may not adequately simulate the complex interaction between frame and infill, and thus, multiple strut models were also utilized in some past literature. Likewise, masonry walls have also been modeled as four-noded shell

elements in between the centerline beam-column elements of the RC frame (Fig. 1e) in many past studies. Some of the past studies, such as Kaushik and Sanganee (2010), Ghaisas et al. (2017), Borah et al. (2021b), Chakra-Varthy and Basu (2021), have carried out linear analysis of CM walls by modeling masonry walls using linear shell elements. Some studies have considered equivalent strut model for the analysis of CM walls; however, their applicability is limited because the considered failure modes in CM walls were quite similar to that considered in masonry infilled frames. Kaushik and Sanganee (2010) estimated a different relation for estimation of the width of the diagonal strut in ESM if it is to be used in case of CM walls. However, the study was limited to calibrating only the lateral stiffness of CM walls with some past experimental studies. Torrisi et al. (2012) and Torrisi and Crisafulli (2017) developed a 12-noded masonry panel element model, which internally includes 6 diagonal struts for nonlinear analysis of infilled RC frame and CM walls, but again similar behavior was assumed for infilled frames and CM walls.

2.4. V-D Strut Model (VDSM)

The V-D (Vertical-Diagonal) strut model (VDSM) is a recently developed modified form of ESM for the analysis of CM structures under the action of both gravity and seismic loads (Borah et al. 2021b). In VDSM, tie-elements of a CM wall are modeled as frame elements and masonry is modeled as a combination of pin-jointed vertical and diagonal strut elements (Fig. 1f). The flexural stiffness of tie-beam is enhanced 20 to 25 times the original stiffness and the width of vertical strut is considered as 75% of the panel length in order to simulate the realistic gravity load distribution in different elements. Thickness of both the struts is taken as the actual wall thickness. Width of the diagonal strut was simply considered as one-third of the length of diagonal strut to match the initial stiffness of CM wall. Nonlinearity can be considered in diagonal struts as well as tie-columns using lumped plasticity approach at specified hinge locations. Nonlinear behavior of tie-columns is simulated using flexure and shear hinges, while axial hinges are defined in the diagonal strut to account for the nonlinearity in masonry walls. Instead of using the masonry prism strength as the axial strength of the diagonal strut, *effective shear strength of masonry* (f_{ss}), which represents the strength corresponding to the weakest failure mode in CM walls, was considered to realistically simulate the failure of masonry walls. Using six independent parameters as uncertain variables, namely, compressive prism strength of masonry ($f_m^{'}$), compressive strength of concrete (f_c), aspect ratio of wall (AR = ratio of the height of the CM wall excluding tie-beam (H_w) to the length of the CM wall excluding tie-columns (L_w)), gravity loads on tie-beams (σ), percentage of reinforcement in tie-columns (ρ_l), and wall thickness (t), empirical equations were developed for estimation of f_{ss} as:

$$f_{ss} = 0.096\, t^{0.217} f_m^{'\,0.827} f_c^{0.081} \rho_l^{0.018} (1 + \sigma)^{0.235} \mathrm{AR}^{0.101} \text{ for AR} \le 1 \quad (7)$$

$$f_{ss} = \frac{0.134\, t^{0.133} f_m^{'\,0.886} f_c^{0.107} \rho_l^{0.002} (1 + \sigma)^{0.004}}{AR^{0.248}} \text{ for AR} > 1 \quad (8)$$

here, f_{ss}, $f_m^{'}$, f_c, σ are in MPa; ρ_l is in %; t is in mm; AR is dimensionless. The effectiveness of the empirical equations and V-D strut model in predicting the lateral load behavior of CM walls was validated in Borah et al. (2021b) using 35 single-bay as well as multi-bay CM wall specimens tested in 14 past studies. The model was able to suitably capture the realistic linear and nonlinear behavior of CM walls with acceptable accuracy.

3. Comparative Assessment Of Modeling Strategies

Aspect ratio of CM walls governs their overall behavior under the action of different loads. Three single-bay, single-story CM walls having different aspect ratios tested previously in half-scale by Borah et al. (2021c) were considered in this section for the comparative assessment of the four modeling strategies discussed in the previous section. The specimens were constructed with burnt-clay bricks in English bond pattern (Fig. 2a). The properties of materials used were: $f_m^{'}$ = 5.2 MPa, E_m = 2000 MPa, f_c = 30.4 MPa, f_{yl} = 549 MPa, and yield strength of transverse rebars, i.e., f_{yt} = 446

MPa. Figure 2 shows other material and geometric properties of the specimens, reinforcement detailing used in tie-members, as well as test set-up and results obtained. The imposed (dead and live) loads applied on the tie-beam of the specimens due to the upper-story was 0.13 MPa. The quasi-static cyclic lateral load tests showed that when AR of masonry panel of a CM wall was reduced from 2.0 to 1.5, the lateral strength of the CM wall increased by about 20%, while it increased by up to 70% when AR was further reduced to 1.0. However, the lateral drift capacity (corresponding to lateral strength) reduced by 43% when the AR was reduced from 2.0 to 1.0. The initiation of cracking in the slender wall S1 was in the form of a flexural crack in tie-column, whereas shear cracks in masonry wall were observed initially for S2 and S3 specimens. In all three walls, initial cracking occurred at around 0.2% lateral drift (i.e., at around 3 mm lateral displacement). The tie-columns of relatively squat specimen S3 suffered the most severe damages and exhibited a sudden drop in strength after reaching the peak. Further, the strain gauge data showed that most longitudinal rebars of tie-columns of all three specimens initially yielded near the bottom at a drift value of 0.5% (i.e., around 7.5 mm lateral displacement), while those at the top started yielding at a much higher lateral drift. Though the initiation of cracks and damage was different in the three specimens, finally, all the specimens failed due to shear failure of tie-columns after masonry suffered severe damage. The obtained hysteretic responses at the end of the tests were converted to idealized trilinear envelopes curves that represent three stages – cracking stage, maximum resistance stage, and ultimate deformation (at 20% strength degradation) stage (Fig. 2d).

The three considered CM walls (Fig. 2) were modeled in SAP2000 using the four modeling strategies explained earlier. Figure 3 shows seven different models developed for the CM wall - S1; similar models were developed for the remaining two CM walls as well. In WCM, the walls were modeled as centerline stick models (beam-column elements) in SAP2000 considering the equivalent masonry cross-section for the RC tie-columns along with increased stiffness of tie-beam. For the basic STM (named as STM-1) and the STM proposed by Tripathy and Singhal (2019) (named as STM-2), walls were converted to pin-jointed trusses and analyzed using the method of joints. For the third type of STM proposed by Rankawat et al. (2021) and named STM-3, walls were modeled in SAP2000 using pin-jointed trusses. In ESM, masonry wall was modeled as a pin-jointed diagonal strut between the beam-column joint of the RC frame as well as discretized shell elements, named as ESM-strut and ESM-shell, respectively. In VDSM, a vertical pin-jointed strut was modeled below the center of the tie-beam in addition to the diagonal strut and increased stiffness of the tie-beam. Important parameters along with the dimensions of different struts calculated for different modeling schemes are given in Table 1. The nonlinear hinge definitions will be discussed in the latter part of this section.

Table 1: Calculated parameters used in different modeling strategies for the specimens S1, S2, and S3.

ID	AR	A_{wc} (mm^2) (WCM)	w_{ds} ($\beta = 12$) (mm) (STM-3)	w_{ds} ($\beta = 3$) (mm) (STM-3)	$w_{ds} = D/4$ (mm) (ESM)	$w_{ds} = D/3$ (mm) (VDSM)	$w_{vs} = 0.75L_w$ (mm) (VDSM)
S1	2.0	524502	1392	1082	448	597	563
S2	1.5	555752	1341	1102	481	642	750
S3	1.0	618252	1483	1297	564	751	1125

3.1 Linear Analysis

All the seven models were first compared by using the linear gravity load analysis results of the CM walls – S1, S2, and S3. Figure 4(a) shows the maximum values of axial forces developed in left and right tie-columns of the specimens obtained from different modeling strategies; whereas Fig. 4(b) shows the axial force values in the masonry wall. As WCM provides the composite behavior of masonry and tie-column, the force distribution in separate elements cannot be obtained. Again, STM-1 and 2 are basically applicable under lateral loading. Thus, the data are blank corresponding to

these models in Figs. 4(a) and 4(b). After the gravity load analyses, the models were also compared using the linear lateral load analysis results as shown in Figs. 4(c) and 4(d) (here the CM walls were analyzed for 45 kN lateral load as the minimum lateral strength of the specimen obtained experimentally was about 47.5 kN). As the STM-2 method was mainly developed for lateral capacity estimation, it is not applicable for estimation of lateral force distribution in CM wall for any other stage. Also, the shell model, i.e. ESM-shell, is not appropriate for the estimation of developed forces in masonry wall of a CM wall under lateral loading, and thus, data corresponding to it is showing blank in Fig. 4(d).

The linear analyses results showed that most of the simplified models failed to capture the gravity load response of CM walls; only ESM-shell and VDSM predicted significant gravity loads in masonry walls representing the true behavior (Fig. 4b). Under lateral loading, STM-1, STM-3, ESM-strut and VDSM were able to predict the developed axial forces in tie-columns as well as masonry walls. It is to be noted here that the other force resultants, such as shear forces and bending moments, in different elements of a CM wall can also be obtained using STM-3, ESM-strut, and VDSM. Thus, only VDSM was found to realistically predict the response of CM walls under both gravity and lateral loads.

3.2 Nonlinear Analysis

To evaluate the effectiveness of the modeling strategies in predicting the nonlinear response of CM walls, nonlinear pushover analyses were carried out on the same CM walls. Nonlinear hinge definitions were assigned in different elements in WCM, STM-3, ESM-strut, and VDSM; the remaining models STM-1, STM-2, and ESM-shell are not capable of simulating nonlinear response of CM walls. In WCM the nonlinearity was defined by a shear hinge near the bottom end of the centerline column. As the shear hinge represents the nonlinearity in the entire CM wall (tie-members as well as masonry wall), lateral force-deformation backbone models developed in the past for CM walls can be used to define the shear hinge properties. A similar concept is also applicable for STM-3, where, the nonlinearity, and hence the hinge definition, is assigned only to the diagonal strut at the center in terms of axial stress-axial strain relationship; tie-members are assumed to remain elastic. This axial hinge definition, which also incorporates the influence of the complete CM wall, can be obtained by converting the lateral force-deformation backbone curve of CM wall to compressive stress-strain backbone curve of diagonal strut. For this, the horizontal component of the axial force in the diagonal strut in STM was considered as the shear force in CM wall (V), and the axial stress was calculated as: $\sigma = V/(t \times w_{ds} \times cos\theta)$; the axial strain ($\varepsilon$) was obtained from the lateral percentage drift (δ) as: $\varepsilon = (\delta \times H_w/100) \times (1/2 \times sin2\theta)$.

The accuracy of the results obtained from both WCM and STM-3 is based on the selection of a particular force-deformation backbone curve model of CM walls. It is difficult to choose a generalized backbone curve model as the existing models were formulated by calibrating experimental responses of CM walls using different sets of parameters that may differ regionally as observed in Borah et al. (2022). The maximum lateral load resistance of CM walls can be predicted by some of the available empirical models with a better confidence level. For example: as per Flores and Alcocer (1996), $V_m = (0.5v_m + 0.3\sigma)A + 0.3 \times 1.26 \times (d_{bl})^2 (f_c f_{yl})^{0.5}$; whereas as per Borah et al. (2022), $V_m = AR^{-0.7}(f_m^{'})^{0.4}(nA_c/A)^{0.9}(1+\sigma)A$; where, V_m is the lateral strength of CM wall, d_{bl} is the diameter of longitudinal bars in tie-columns, and n is the number of tie-columns. Next, the cracking lateral load and lateral load at ultimate drift are functions of lateral strength only (about 70–80% of lateral strength, respectively). However, the drift capacity estimation at different stages is not an easy task because of the high level of uncertainty in deformation prediction in the nonlinear range. Flores and Alcocer (1996) and Riahi et al. (2009) suggested to consider the lateral drift at cracking (δ_{cr}) obtained from the lateral stiffness (i.e., the slope of the load-deformation curve) after knowing the cracking load. As per Flores and Alcocer (1996), the lateral drift at maximum lateral load (δ_m) and ultimate load (δ_u) can be simply considered as 0.3% and 0.5%, respectively. On the other hand, Borah et al. (2022) suggests: $\delta_{cr} = AR^{0.125}(f_m^{'})^{-0.983}$; $\delta_m = 1.5AR\delta_{cr}$; $\delta_u = 2\delta_m$. To understand the influence of variation in the backbone curve models in more detail, the lateral strengths and lateral drifts of the three CM walls were predicted using several available empirical models and compared in Tables 2 and 3, respectively.

Table 2
Experimentally obtained and empirically predicted lateral strength (kN) of the considered CM walls.

ID	Exp	Bor	M&L3	M&L2	S&R	M&L1	Ria	Bzm1	Bzm2	Bzm3	M&C	T&K	F&A
		2022	2019	2019	2014	2013	2009	2008	2008	2008	2006	1997	1996
S1	**47.5**	48	97	30	51	37	34	60	77	57	104	61	33
S2	**55.8**	60	105	39	68	46	43	70	86	66	112	70	40
S3	**81.1**	83	119	58	102	63	60	120	157	112	126	140	56

Bor = Borah et al. (2022); M&L3 and M&L2 = Marques and Lourenço (2019); S&R = Singhal and Rai (2016); M&L1 = Marques and Lourenço (2013); Ria = Riahi et al. (2009); Bzm1, Bzm2, Bzm3 = Bourzam et al. (2008a); M&C = Marinilli and Castilla (2004); T&K = Tomaževič and Klemenc (1997); F&A = Flores and Alcocer (1996).

Table 3
Experimentally obtained and empirically predicted lateral drifts (%) of the considered CM walls.

ID	δ_{cr}					δ_m				δ_u			
	Exp	Bor 2022	Ria 2009	F&A β = 12 1996	F&A β = 3 1996	Exp	Bor 2022	Ria 2009	F&A 1996	Exp	Bor 2022	Ria 2009	F&A 1996
S1	**0.20**	0.22	0.11	0.05	0.13	**0.87**	0.65	0.44	0.30	**1.75**	1.29	0.67	0.50
S2	**0.20**	0.21	0.11	0.05	0.09	**0.82**	0.47	0.44	0.30	**2.38**	0.94	0.67	0.50
S3	**0.20**	0.20	0.11	0.04	0.06	**0.50**	0.30	0.44	0.30	**0.98**	0.59	0.67	0.50

The empirically predicted lateral strength and drifts as given in Tables 2 and 3 clearly show that the values obtained using Borah et al. (2022) are closer to the experimental observations; therefore, the empirical model developed by Borah et al. (2022) was used for generating the nonlinear hinge properties for diagonal struts in WCM as well as STM-3. In addition, as the model of F&A has been used popularly in past literature, it was also included for further comparative investigation. Figure 5 shows all the developed hinge properties for WCM and STM-3. The drift estimation at cracking stage using F&A involves stiffness of wall that depends on the boundary condition factor β (= 3 or 12). Again, hinge definition in the diagonal strut of STM involves shear stress that is obtained by dividing the predicted shear force by the cross-sectional area of the strut (i.e., it depends on the width of strut and in turn stiffness and β). Thus, two sets of hinge definitions (using Borah et al. (2022) and F&A for two values of β) were considered in the study for WCM and STM-3 as shown in Fig. 5.

In ESM-strut and VDSM, nonlinear behavior in the form of plastic hinges was defined in the diagonal strut as well as the RC tie-columns (Figs. 6 and 7). Nonlinearity was not considered in the tie-beams as no damage was observed in the tie-beams in the tests. For the diagonal struts, axial hinge properties were defined considering $f_m^{'}$ (3 MPa) for ESM, and f_{ss} (1.33 MPa, 1.43 MPa, and 1.44 MPa for S1, S2, and S3, respectively) for VDSM as shown in Fig. 6. Further, ASCE 41 − 13 (ASCE 2017) was used to define the flexural hinge properties for tie-columns, while brittle shear hinges were defined in tie-columns using the material strengths from relevant Indian standards.

The lateral load-displacement responses of the walls obtained from the pushover analyses are compared with the experimentally obtained idealized backbone curves of the specimens in Fig. 7. The comparison study showed that the models WCM and STM-3 predicted the lateral load response well when the nonlinearity was defined using the backbone curve model of Borah et al. (2022). On the other hand, using the backbone curve model of Flores and Alcocer (1996) for nonlinearity definition resulted in underprediction of the lateral load response from both WCM and STM-3 models.

Further, ESM highly overpredicted the lateral load responses of all CM walls as the model considers the strength of wall based on the prism compressive strength of masonry in the nonlinearity definition of diagonal strut. However, VDSM considers the strength corresponding to the weakest failure mode of masonry by using f_{ss} in the nonlinearity definition of diagonal strut, and thus, predicted the lateral load responses of CM wall quite well. Analysis results from VDSM showed that the first nonlinearity that occurred in all CM wall models was in the masonry walls followed by the hinge formation in the tie-columns. As observed experimentally too, failure also occurred in the masonry walls first. Though WCM, STM-3, and VDSM all predicted the lateral strength reasonably well, only VDSM can predict the failure in RC tie-members in addition to predicting it in the masonry wall. This is because both WCM and STM-3 model the collective nonlinearity of tie-members and masonry walls, and not separately.

The discussed results showed the applicability and comparison of the four modeling strategies WCM, STM-3, ESM–strut, and VDSM for nonlinear analysis of CM walls. Sometimes, assessment of only lateral strength is sufficient for preliminary seismic design instead of evaluation of complete nonlinear response. The effectiveness of all the seven methodologies in lateral strength prediction was evaluated and compared with the experimentally obtained strengths for the three CM walls as shown in Fig. 8. Though STM-1 and STM-2 strategies are not software-based, they may be utilized for limit-based analysis. The blank spaces in Fig. 8 corresponding to STM-1 signify that the lateral capacity of CM walls cannot be predicted using the basic strut-and-tie methodology as the number of unknowns was more than the number of available equilibrium equations. As discussed earlier, the lateral capacity of CM walls was obtained using STM-2 by either considering yielding of longitudinal reinforcement in tie-columns or taking the limiting strut capacity. Thus, using STM-2, the axial forces in the diagonal strut were obtained as 71 kN, 77 kN, and 90 kN for S1, S2, and S3, respectively, if yielding of rebars was considered. However, the limiting capacity for the diagonal strut (F_{ss}) was found to be 194 kN, 208 kN, and 227 kN for S1, S2, and S3, respectively, which were significantly higher. Thus, considering the minimum of the two, the lateral capacity of CM walls was obtained as 35 kN, 45 kN, and 65 kN for S1, S2, and S3, respectively, signifying that STM-2 underpredicts the lateral capacity of CM walls. ESM-shell is also not suitable for strength assessment in simplified analysis carried out in SAP2000; therefore, the lateral strength values corresponding to it are not shown in Fig. 8. The empirically predicted lateral strength values of the three CM walls (as given in Table 2) are also shown in Fig. 8 to demonstrate the influence of a particular strength or backbone model in the calibration of lateral strength using WCM or STM-3. As already discussed, the strength prediction from WCM and STM-3 is a direct function of the backbone model used; hence the prediction was better when Borah et al. (2022) backbone curve was used. But both WCM and STM-3 cannot be always relied upon in absence of an accurate backbone curve model. Further, ESM prediction was obviously very conservative as it considers only the masonry compressive prism strength as the strength of masonry walls. Among all the models, VDSM consistently provides a good prediction of strength even without using a representative combined backbone curve model of the CM walls.

4. Applicability Of Different Modeling Strategies For Multistory Cm Buildings

After understanding the pros and cons of existing modeling strategies in predicting the lateral load response of single storey CM walls, it is also important to evaluate the application of the existing modeling strategies for multistory CM buildings. The building selected for the case study was a three-story residential building in a highly seismic-prone region. The 16 m long and 9 m wide building was symmetric about the Y-axis as shown in Fig. 9. Height of each floor was 3 m taking the total height to 9 m. Important material properties and dimensions for the key structural elements are provided in Table 4. In absence of an established design code for CM buildings in India, international practices (Meli et al. 2011) were followed for the preliminary design. The thickness of the walls (t) was taken as 150 mm ensuring the slenderness ratio (H_w/t) to be less than the limit of 30. RC tie-columns of size 150 mm × 150 mm were provided as their minimum dimension is generally taken equal to the masonry wall thickness. RC tie-beams of size 150 mm × 150 mm were provided

and thickness of RC slabs was taken as 125 mm. The tie elements were reinforced with 4 numbers of 10 mm diameter longitudinal rebars and 6 mm diameter stirrups at 150 mm center-to-center spacing.

Table 4
Considered material properties and dimensions of structural elements.

Material Properties	Compressive strength of masonry prism (f'_m)	3 MPa
	Modulus of elasticity of masonry ($E_m = 550f'_m$)	1650 MPa
	Compressive strength of concrete (f_c)	25 MPa
	Modulus of elasticity of concrete (E_c)	25000 MPa
	Yield strength of longitudinal rebars (f_{yl})	415 MPa
	Yield strength of transverse rebars (f_{yt})	250 MPa
	Modulus of elasticity of steel (E_s)	2×10^5 MPa
Dimensions and Detailing	CM wall height	3 m
	CM wall thickness	150 mm
	RC floor/roof slab thickness	125 mm
	Cross-section of tie elements	150 mm × 150 mm
	Longitudinal reinforcement in tie elements	4 bars of 10 ϕ
	Transverse reinforcement in tie elements	6 ϕ at 150 mm c/c

For the analysis of the building, dead loads and live loads were considered based on relevant Indian Standards (BIS 1987). Thus, superimposed dead load in the building was considered as 1.5 kN/m^2 and live load was considered as 2 kN/m^2. Four different models, i.e., WCM, STM-3, ESM-strut, and VDSM, were developed for the building; STM-1, STM-2, and ESM-shell were not considered as these models cannot be used to carry out the nonlinear pushover analysis. Small openings in masonry walls (area less than 10% of the total masonry wall area) were disregarded and those walls were modeled as solid walls. On the other hand, for the masonry walls having larger openings (such as doors), the walls were disregarded in that panel. The RC floor slabs were modeled as linear shell elements in all the four modeling strategies. The building comprises mainly of four types of CM walls with four different aspect ratios – 2.17, 1.1, 0.87, and 0.76; and based on the center-to-center length, these walls were named as wall-1500, wall-2800, wall-3500, and wall-4000, respectively. The estimated values of the important parameters required for modeling these four CM walls are provided in Table 5.

As discussed in the Section 3, the lateral load-deformation prediction using WCM and STM-3 is based on the selection of empirical strength and deformation equations for nonlinear hinge definition. The key controlling parameter for the hinge definition in WCM and STM-3 is the lateral strength. Though the previous section showed the suitable empirical models by comparing with experimental observations, generalization of a particular empirical model may not always provide the actual realistic response. Thus, the variation of predicted lateral strength using any of the empirical models are again compared in Fig. 10 for the four CM walls of the case study building. It was observed that the results can be divided into two groups of empirical models. The first group contains the empirical models - Bor, M&L2, M&L1, and F&A; and the second group contains the remaining empirical models – M&L3, S&R, Ria, Bzm1, Bzm2, Bzm3, M&C, T&K. The empirical models of the second group estimated significantly higher values in comparison to the first for all the walls. For wall-

1500, the strength prediction by the second group was about 80–90% more of that predicted by the first group. Similarly, the second group predicted about 50% more strength for wall-2800. And for wall-3500 and wall-4000, the lateral strength predicted by the second group was about twice of that predicted by the first group. Among the considered empirical models the empirical model developed by Borah et al. (2022) predicts the lateral strength with consistent accuracy as also observed in section 3.2. Clearly, the empirical models in the first group (Bor, M&L2, M&L1, and F&A) can be considered to be more reliable for strength prediction of the considered CM building.

Table 5
Calculated parameters used in different modeling strategies for the case study building.

ID	A_{wc} (mm^2) (WCM)	w_{ds} (mm) (STM-3)	$w_{ds} = D/4$ (mm) (ESM-strut)	$w_{ds} = D/3$ (mm) (VDSM)	$w_{vs} = 0.75L_w$ (mm) (VDSM)	f_{ss} (MPa) (VDSM)
wall-1500	884318	2593	839	1118	1013	0.806
wall-2800	1079318	2624	1026	1368	1988	0.953
wall-3500	1184318	2996	1152	1537	2513	0.962
wall-4000	1259318	3355	1250	1667	2888	0.948

Therefore, for the further analysis of the case study building with WCM and STM-3, only the empirical strength prediction model of Borah et al. (2022) was considered, as it provided a better prediction of lateral capacity of the other CM walls (Table 2). The lateral load at cracking and ultimate loads were considered to be 80% of the lateral strength. The prediction of lateral deformation capacity for masonry structures is anyway a very challenging task, and thus, both the method - Flores and Alcocer (1996) and Borah et al. (2022) were considered for displacement prediction. Thus, two types of backbone curve with two different displacement profile and same lateral load profile were developed for a particular wall for plastic hinge definition. Hinge-1 corresponds to the displacement profile of Flores and Alcocer (1996); whereas Hinge-2 corresponds to the displacement profile of Borah et al. (2022). Figure 11 shows these two types of hinges for WCM and STM-3. As observed in the figure, Hinge-1 (h1) gives constant displacement values for all the walls; however, Hinge-2 (h2) gives different displacement profiles for walls with different aspect ratios. Again, for the axial hinge definition in the diagonal strut in ESM, the masonry stress-strain model developed by Kaushik et al. (2007) was used. Similar to this, the axial hinge profiles for the diagonal strut in VDSM were developed considering the estimated values of f_{ss} (Table 5) as shown in Fig. 11. In addition, flexural hinges were defined for the tie-columns in ESM and VDSM. Considering the mentioned geometrical and material property details, WCM, STM-3, ESM-strut, and VDSM were developed for the case study CM building. For example, Fig. 12 shows the developed VDSM of the case study building. Nonlinear pushover analyses were carried out for the building considering all the four developed modeling strategies, in X and Y directions.

The lateral load-displacement responses of the case study building obtained from the pushover analyses using the four different modeling strategies are shown in Fig. 13. The figure clearly shows that as expected the ESM predicted very high lateral strength (around 4700 kN) as well as high lateral deformability of the CM building in comparison to other types. The other three types of modeling strategies, i.e., WCM, STM-3, and VDSM estimated lateral strength of around 1400 kN to 2000 kN.

The outputs of WCM and STM-3 were almost similar as these models were based on a similar set of nonlinear hinge definitions obtained from the global responses of the CM walls of the building. The lateral strength of the CM building was 1400 kN to 1500 kN for WCM and STM-3 when the hinge definition was assigned with the empirical lateral strength model of Borah et al (2022). The two types of hinges - h1 and h2 - considered in WCM and STM-3 changes the lateral

deformability behavior of the building. The predicted lateral deformability of the CM building from WCM and STM-3 was lesser with h1 hinge in comparison to that with h2 hinge. The maximum deformability of the building was around 10 mm to 20 mm with h1 hinge (i.e., deformation model of Flores and Alcocer (1996)); while it was around 30 mm to 40 mm with h2 hinge (i.e., deformation model of Borah et al. (2022)) when WCM and STM-3 were utilized.

Unlike WCM and STM-3, where the complete lateral load behavior of the entire wall is required as input, the hinge definition in VDSM is based on actual material properties. Therefore, the obtained lateral load response from VDSM was found to be not similar to that obtained from WCM or STM-3. The lateral capacity of the building using VDSM was around 2000 kN, and the maximum lateral deformability was observed to be around 40 mm. Further, the analysis of the building with VDSM showed that the first nonlinearity or hinge formation was in the masonry walls followed by the hinge formation in the tie-columns, which is generally expected in case of a CM structure. However, analysis with ESM showed the reverse hinge formation results (i.e., first in tie-columns, and later in masonry walls) both in case of the building as well as single bay CM walls in section 3. Again, as STM-3 does not consider nonlinearity in tie-columns, hinge formation can be seen in masonry walls (i.e., diagonal struts) only. Lastly, as WCM considers the collective nonlinearity behavior of tie columns and masonry wall by modeling the CM wall as a single element; the separate failure or hinge formation cannot be observed. This comparison clearly shows the superiority of the VDSM model over the other modeling techniques for nonlinear analysis of CM walls using which the force resultants in tie-members can also be estimated along with the prediction of the damage and failure patterns in different members and the global load-deformation behavior.

5. Summary And Conclusion

The prediction of structural response of anisotropic, brittle materials, such as masonry, is often very challenging using simplified models. The available modeling strategies have potential to simulate only some of the structural responses of confined masonry wall. The modeling strategies consider different assumptions, provide results with different levels of accuracy, and carry different limitations. Some analysis methods consider simple mathematical tools based on the equilibrium of forces at a joint, while some have been transferred into commercial software packages, making them available to engineers. The software-based numerical models have the superiority as software allows to define the geometric details, nonlinearity, and variety of choices to perform linear and nonlinear analyses. It was observed that the application of the basic strut-and-tie method (STM-1) is limited to determination of force resultants in members of the walls when the applied lateral load is provided and structure is determinate. The lateral capacity may be estimated from STM (STM-2) by reducing one unknown considering yielding of rebars or from limiting capacity of strut. However, these STM strategies are not much helpful to predict other nonlinear responses of the structure, such as lateral load - lateral deformation profile. Further, WCM provides the opportunity to calibrate the nonlinear response of CM structures using the global response of CM wall. However, the hypothesis of monolithic behavior assumed in WCM does not provide the opportunity to study the individual behavior of tie-columns and complex force transmission in different elements under loading. In fact, the concept of monolithic behavior of masonry wall and tie-columns is mainly valid to represent the elastic response at the initial stage.

To overcome such issues, STM was extended (STM-3) for nonlinear analysis in a commercial software where the global CM wall behavior is used for the nonlinearity definition in the diagonal strut. Though the strategy manages to analyze the nonlinear lateral load-deformation response of CM wall just like WCM, this strategy is still not useful to study the individual behavior of the tie-columns and masonry wall as it considers the global CM wall behavior in the masonry wall portion. In addition, no nonlinear definition is considered for the tie-columns; whereas many past damage reports showed that tie-columns suffer significant cracks and failure of CM wall occurs with the failure of tie-columns after significant damages in masonry wall. Moreover, selection of a reliable existing backbone model or the empirical models for backbone parameters of CM wall (stiffness, strength, and deformation) for nonlinearity definition in WCM or STM-3 is

equally important as these models replicate the same global behavior. The conventional diagonal ESM has been utilized in CM structures mainly for linear analysis. None of these models have the capability to realistically simulate the gravity load transfer from the tie-beams to the masonry walls. The model VDSM has the potential to realistically simulate both gravity and lateral load responses of CM walls. Further, the model also provides the opportunity to study the developed forces in the tie-columns separately in different loading stages by considering separate nonlinearity definitions for tie columns and diagonal strut.

Different modeling strategies were compared in this article using force-based as well as displacement-based assessment. From a preliminary linear gravity load analysis of single-story CM walls using different modeling strategies, it was observed that the equivalent frame model for the RC tie frame along with shell elements for masonry wall (ESM-shell), and V-D strut model (VDSM) are the only models that capture the contribution of masonry wall in gravity load distribution. On the other hand, for linear lateral load analysis, the strut and tie model (STM-1 and STM-3), equivalent strut model (ESM-strut), and V-D strut model (VDSM) provide the opportunity to study the developed forces in the members of the wall. A comparative study of the different modeling strategies was carried out for the single-story CM walls with different aspect ratios, whose lateral load responses were already studied under cyclic lateral load tests. The results obtained from the nonlinear pushover analyses showed that the wide column model (WCM) and STM-3 very well predict the lateral load responses if a proper empirical backbone model is selected for nonlinear hinge definition. The hinge definition in WCM and STM-3 using the empirical model of Borah et al. (2022) provides results closer to experimentally obtained results. VDSM also predicted the lateral load-deformation response of the CM walls with a slight overprediction of strength, but more importantly, VDSM does not need any empirical backbone model for the CM walls for nonlinear hinge definition. Applicability of all the models in the analysis of multistory CM building was examined in the study and it was found that the WCM, STM-3, and VDSM have the potential to successfully predict the lateral load-deformation responses. The study showed that VDSM provides the opportunity to replicate the failure pattern of typical CM structure. Further, reliable prediction of developed forces in different elements of the building can be done by conducting nonlinear analysis using VDSM.

Declarations

Funding

Authors gratefully acknowledge the Grant received from the Science and Engineering Research Board, Department of Science and Technology, Government of India (Grant No. ECR/2018/000489).

Competing Interests

The authors have no relevant financial or non-financial interests to disclose.

Author Contributions

The study was conceptualized and designed by Bonisha Borah, and she carried out all the analysis reported in the manuscript. Resources and supervision were provided by Hemant B Kaushik and Vaibhav Singhal. The first draft of the manuscript was written by Bonisha Borah and all authors commented on previous versions of the manuscript. All authors have read and approved the final manuscript.

Data Availability

The datasets generated during and/or analysed during the current study are available from the corresponding author on reasonable request.

References

1. Ahmad, N., Ali, Q., Ashraf, M., Khan, A. N., & Alam, B. (2012). “Performance assessment of low–rise confined masonry structures for Earthquake induced ground motions.” *International Journal of Civil & Structural Engineering*, 2(3), 851-868.
2. Amouzadeh Tabrizi, M., and Soltani, M. (2017). “In-plane response of unreinforced masonry walls confined by reinforced concrete tie-columns and tie-beams.” *Advances in Structural Engineering*, 20(11), 1632-1643.
3. ASCE (2017). ASCE/SEI 41-17: Seismic evaluation and retrofit rehabilitation of existing buildings. American Society of Civil Engineers.
4. BIS (1987). Code of Practice for Design Loads (Other Than Earthquake) for Buildings and Structures. Part 2: Imposed Loads. IS875-Part 2. Second Revision, Bureau of Indian Standards, New Delhi.
5. Borah, B., Kaushik, H.B., and Singhal, V. (2020), “Finite Element Modelling of Confined Masonry Wall under In-plane Cyclic Load.” IOP Conf. Series: Materials Science and Engineering, Vol 936 (1), IOP Publishing.
6. Borah, B., Kaushik, H.B., and Singhal, V. (2022), “Lateral Load-Deformation Models for Seismic Analysis and Performance-based Design of Confined Masonry Walls.” *Journal of Building Engineering*, Vol 48, May 2022, Elsevier, 103978.
7. Borah, B., Singhal, V., and Kaushik, H.B. (2019). “Sustainable housing using confined masonry buildings.” SN Applied Sciences, 1:983, Springer Nature.
8. Borah, B., Singhal, V., and Kaushik, H.B. (2021a), “Assessment of Important Parameters for Seismic Analysis and Design of Confined Masonry Buildings: A Review.” Advances in Structural Technologies, Chapter 20, Lecture Notes in Civil Engineering, Adhikari S., Dutta A., Choudhury S. (eds.), Springer, Singapore, 261-275.
9. Borah, B., Kaushik, H.B., and Singhal, V. (2021b). “Development of a Novel V-D Strut Model for Seismic Analysis of Confined Masonry Buildings.” Journal of Structural Engineering, Vol 147(3), March 2021, ASCE, 04021001.
10. Borah, B., Singhal, V., and Kaushik, H.B. (2021c). “Assessment of Seismic Design Provisions for Confined Masonry using Experimental and Numerical Approaches.” Engineering Structures, Vol 245, 15 October 2021, Elsevier, 112864.
11. Bourzam, A., Ikemoto, T., and Miyajima, M. (2008a). “Lateral resistance of confined brick wall under cyclic quasi-static lateral loading.” *Proc., 14th World Conference on Earthquake Engineering*, Beijing, China.
12. Brzev, S. (2007). *Earthquake-resistant confined masonry construction (First Edition)*. National Information Center of Earthquake Engineering (NICEE), Indian Institute of Technology Kanpur, India.
13. Brzev, S. and Mitra, K. (2018). *Earthquake-resistant confined masonry construction (Third Edition)*. National Information Center for Earthquake Engineering (NICEE), Indian Institute of Technology Kanpur, India
14. Brzev, S., and Pérez Gavilán, J. J. (2016). “Application of strut-and-tie model for seismic design of confined masonry shear walls.” *Proc., 16th International Brick and Block Masonry Conference, Padova, Italy.*
15. Chakra-Varthy, P., & Basu, D. (2021). Natural period and vertical distribution of base shear in confined masonry buildings using ambient vibration test. Bulletin of Earthquake Engineering, 19(4), 1851-1899.
16. Flores L., and Alcocer S.M. (1996). “Calculated response of confined masonry structures.” *Proc., 11th World Conference on Earthquake Engineering*, paper no. 1830, Acapulco, Mexico.
17. Galvis, F. A., Miranda, E., Heresi, P., Dávalos, H., & Ruiz-García, J. (2020). “Overview of collapsed buildings in Mexico City after the 19 September 2017 (Mw7. 1) earthquake.” *Earthquake Spectra*, 36(S2), S83-S109.

18. Ghaisas, K. V., Basu, D., Brzev, S., and Gavilán, J. J. P. (2017). "Strut-and-Tie Model for seismic design of confined masonry buildings." *Construction and Building Materials*, 147, 677-700.
19. Holmes, M., (1961). "Steel frames with brickwork and concrete infilling." *Proc., Institute of Civil Engineers*, 19 (2), 473-478.
20. Janaraj, T., and Dhanasekar, M. (2014). "Finite element analysis of the in-plane shear behavior of masonry panels confined with reinforced grouted cores." *Construction and Building Materials*, 65, 495-506.
21. Kappos, A. J., Penelis, G. G., and Drakopoulos, C. G. (2002). "Evaluation of simplified models for lateral load analysis of unreinforced masonry buildings." *Journal of Structural Engineering*, 128(7), 890-897.
22. Kaushik, H. B., Rai, D. C., and Jain, S. K. (2007). "Stress-Strain Characteristics of Clay Brick Masonry under Uniaxial Compression." *Journal of Materials in Civil Engineering*, 19 (9), 728-739.
23. Kaushik, H. B., Rai, D. C., and Jain, S. K. (2009), "Effectiveness of some strengthening options for masonry-infilled RC frames with open first story." *Journal of Structural Engineering*, ASCE, 135(8), 925-937.
24. Kaushik, H.B., and Sanganee, D.A. (2010). "Analytical investigations of confined masonry constructions." *Proc., 3rd International Earthquake Symposium*, Bangladesh University of Engineering and Technology, Dhaka, Bangladesh, and Bangladesh Earthquake Society, 223-230.
25. Lagomarsino, S., Penna, A., Galasco, A., and Cattari, S. (2013). "TREMURI program: an equivalent frame model for the nonlinear seismic analysis of masonry buildings." *Engineering Structures*, 56, 1787-1799.
26. Marinilli, A., and Castilla, E. (2004). "Experimental evaluation of confined masonry walls with several confining-columns." *Proc*., *13th World Conference on Earthquake Engineering*, paper no. 2129, Vancouver, British Columbia, Canada.
27. Marques, R., and Lourenço, P. B. (2013). "A model for pushover analysis of confined masonry structures: implementation and validation." *Bulletin of Earthquake Engineering*, 11(6), 2133-2150.
28. Marques, R., and Lourenço, P. B. (2019). "Structural behaviour and design rules of confined masonry walls: Review and proposals." *Construction and Building Materials*, 217, 137-155.
29. Marques, R., Pereira, J. M., & Lourenço, P. B. (2020). "Lateral in-plane seismic response of confined masonry walls: From numerical to backbone models." *Engineering Structures*, 221, 111098.
30. Medeiros, P., Vasconcelos, G., Lourenço, P. B., and Gouveia, J. (2013). "Numerical modeling of non-confined and confined masonry walls." *Construction and Building Materials*., 41, 968-976.
31. Meli, R., Brzev, S., Astroza, M., Boen, T., Crisafulli, F., Dai, J., Farsi, M., Hart, T., Mebarki, A., Moghadam, A. S., and Quinn, D. (2011). *Seismic design guide for low-rise confined masonry buildings*. Publication WHE – 2011 – 02, World Housing Encyclopedia, Earthquake Engineering Research Institute (EERI), Oakland, California.
32. NTC-M (2004). *Complementary Technical Norms for Design and Construction of Masonry Structures*. Mexico City Building Code, Gaceta Oficial del Distrito Federal, Mexico.
33. Okail, H., Abdelrahman, A., Abdelkhalik, A., and Metwaly, M. (2016). "Experimental and analytical investigation of the lateral load response of confined masonry walls." *HBRC journal*, 12(1), 33-46.
34. Paulay, T., and Priestley, M. J. N. (1992). *Seismic design of reinforced concrete and masonry buildings*. Wiley-Interscience, New York.
35. Polyakov, S. V., (1956). *Masonry in framed buildings: An investigation into the strength and stiffness of masonry infilling*. Published by Gosudarstvennoe izdatel'stvo literatury po stroitel'stvu i arkhitekture, Moscow (Translation into English by G. L. Cairns).
36. Rangwani, K., & Brzev, S. (2017). "Seismic analysis of confined masonry shear walls using the wide column model." *Applied Mechanics and Materials*, 857, 212-218, Trans Tech Publications Ltd.

37. Ranjbaran, F., Hosseini, M., & Soltani, M. (2012). “Simplified formulation for modeling the nonlinear behavior of confined masonry walls in seismic analysis.” *International Journal of Architectural Heritage*, 6(3), 259-289.
38. Rankawat, N., Brzev, S., Jain, S. K., and Gavilan, J. J. P. (2021). “Nonlinear seismic evaluation of confined masonry structures using equivalent truss model.” *Engineering Structures*, 248, 113114.
39. Riahi, Z., Elwood, K. J., and Alcocer, S. M. (2009). “Backbone model for confined masonry walls for performance-based seismic design.” *Journal of Structural Engineering*, 135(6), 644-654.
40. Schlaich, J., Schäfer, K., & Jennewein, M. (1987). Toward a consistent design of structural concrete. PCI journal, 32(3), 74-150.
41. Singhal, V., and Rai, D. C. (2016). “In-plane and out-of-plane behavior of confined masonry walls for various toothing and openings details and prediction of their strength and stiffness.” *Earthquake Engineering and Structural Dynamics*, 45(15), 2551-2569.
42. Smoljanović, H., Živaljić, N., Nikolić, Ž., and Munjiza, A. (2017). “Numerical model for confined masonry structures based on finite discrete element method.” *International Journal for Engineering Modeling*, 30(1-4), 19-35.
43. Stafford-Smith, B., (1962). “Lateral stiffness of infilled frames.” *Journal of Structural Division*, ASCE, Vol. 88, No. 6, December, pp. 183-199.
44. Terán-Gilmore, A., Zuñiga-Cuevas, O., and Ruiz-García, J. (2009). “Displacement-based seismic assessment of low-height confined masonry buildings.” *Earthquake Spectra*, 25(2), 439-464.
45. Tomaževič, M., & Klemenc, I. (1997a). “Seismic behaviour of confined masonry walls.” *Earthquake Engineering and Structural Dynamics*, 26(10), 1059-1071.
46. Torrisi, G. and Crisafulli, F. (2017). “Computational implementation of an improved masonry panel element.” *Proc., 16th World Conference on Earthquake Engineering, Santiago, Chile*.
47. Torrisi, G.S., Crisafulli, F.J. and Pavese, A. (2012). “An innovative model for the in-plane nonlinear analysis of confined masonry and infilled frame structures.” *Proc., 15th World Conference on Earthquake Engineering,* pp. 24-28.
48. Tripathy, D., and Singhal, V. (2019). “Estimation of in-plane shear capacity of confined masonry walls with and without openings using strut-and-tie analysis.” *Engineering Structures*, 188, 290-304.
49. Wight, J. K., and MacGregor, J. G. (2005). Reinforced concrete: Mechanics and design. Fifth Edition. Upper Saddle River, NJ: Prentice Hall.
50. Yacila, J., Camata, G., Salsavilca, J., and Tarque, N. (2019). “Pushover analysis of confined masonry walls using a 3D macro-modelling approach.” *Engineering Structures*, 201, 109731.

Figures

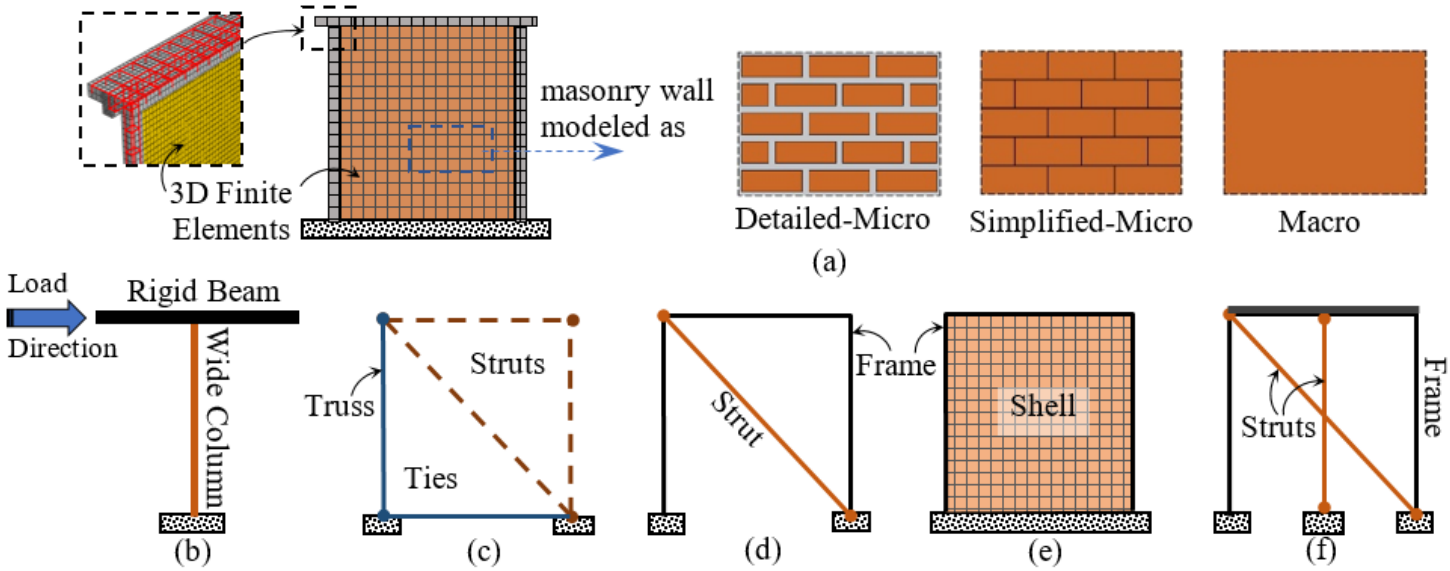

Figure 1

Schematic of 3D and 2D modeling strategies for CM wall: (a) FEM, (b) WCM, (c) STM, (d) ESM-strut, (e) ESM-shell, and (f) VDSM.

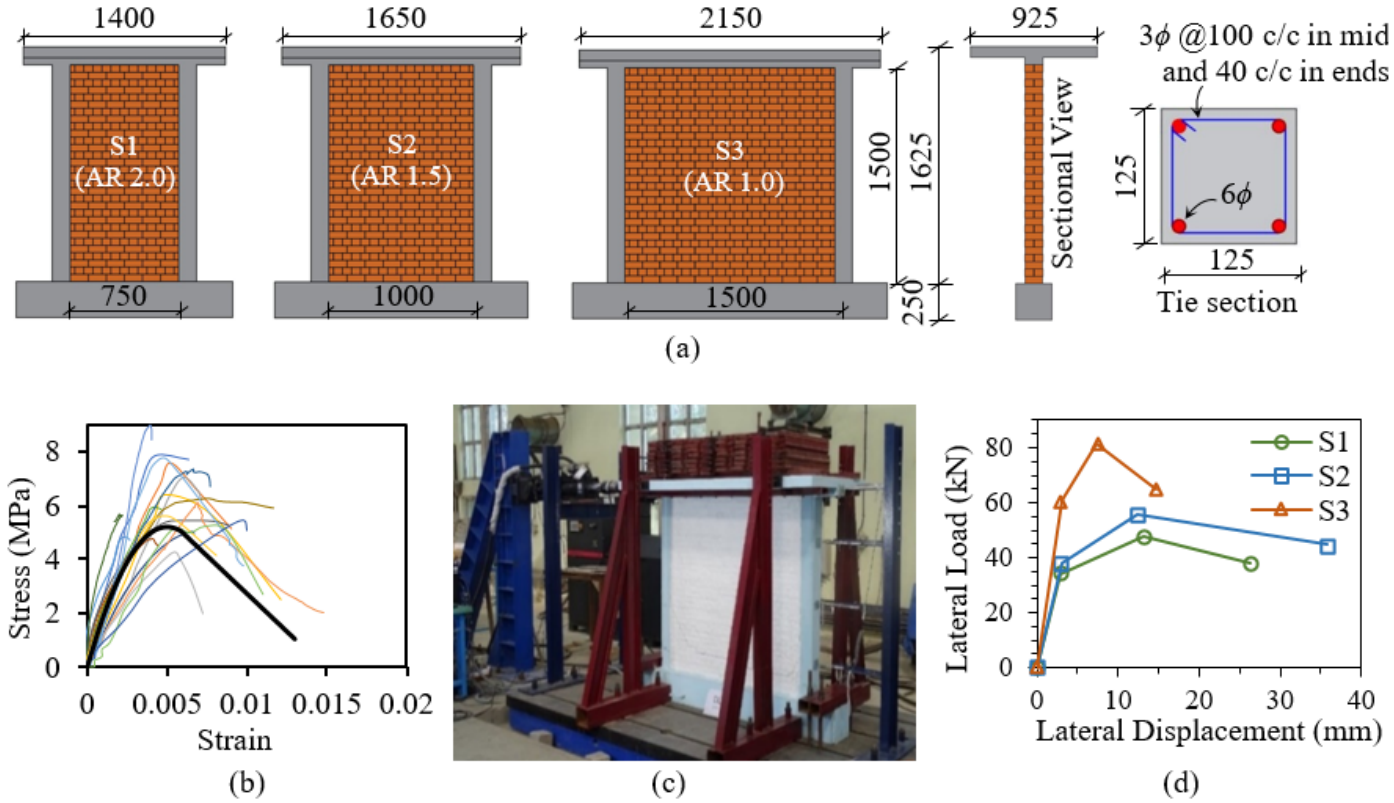

Figure 2

Details of experimental study: (a) Geometric and reinforcement detailing of specimens (all dimensions are in mm), (b) Masonry prism test results, (c) Test set-up, and (d) Idealized backbone curves.

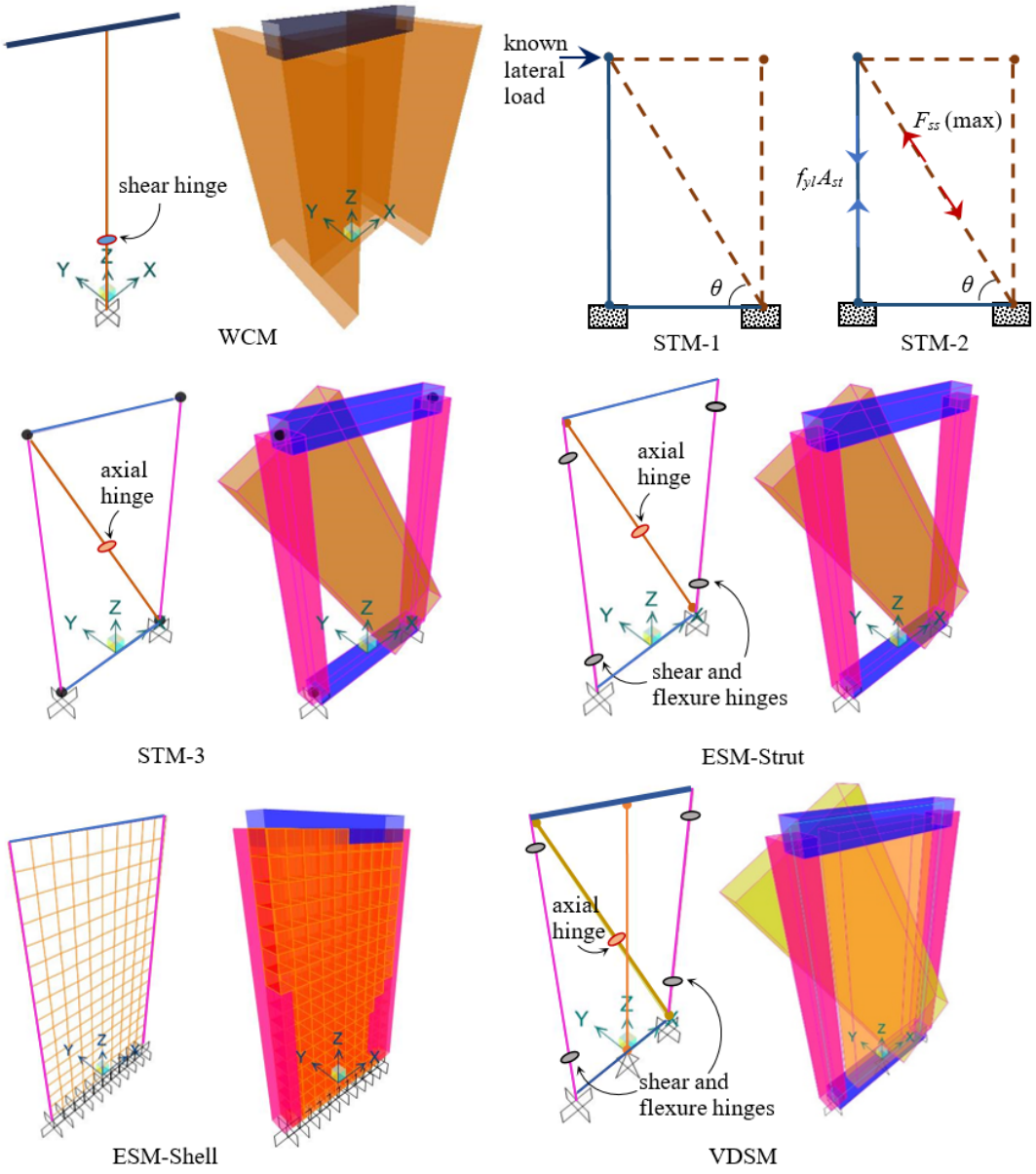

Figure 3

Different modeling strategies for the analysis of the considered CM wall S1.

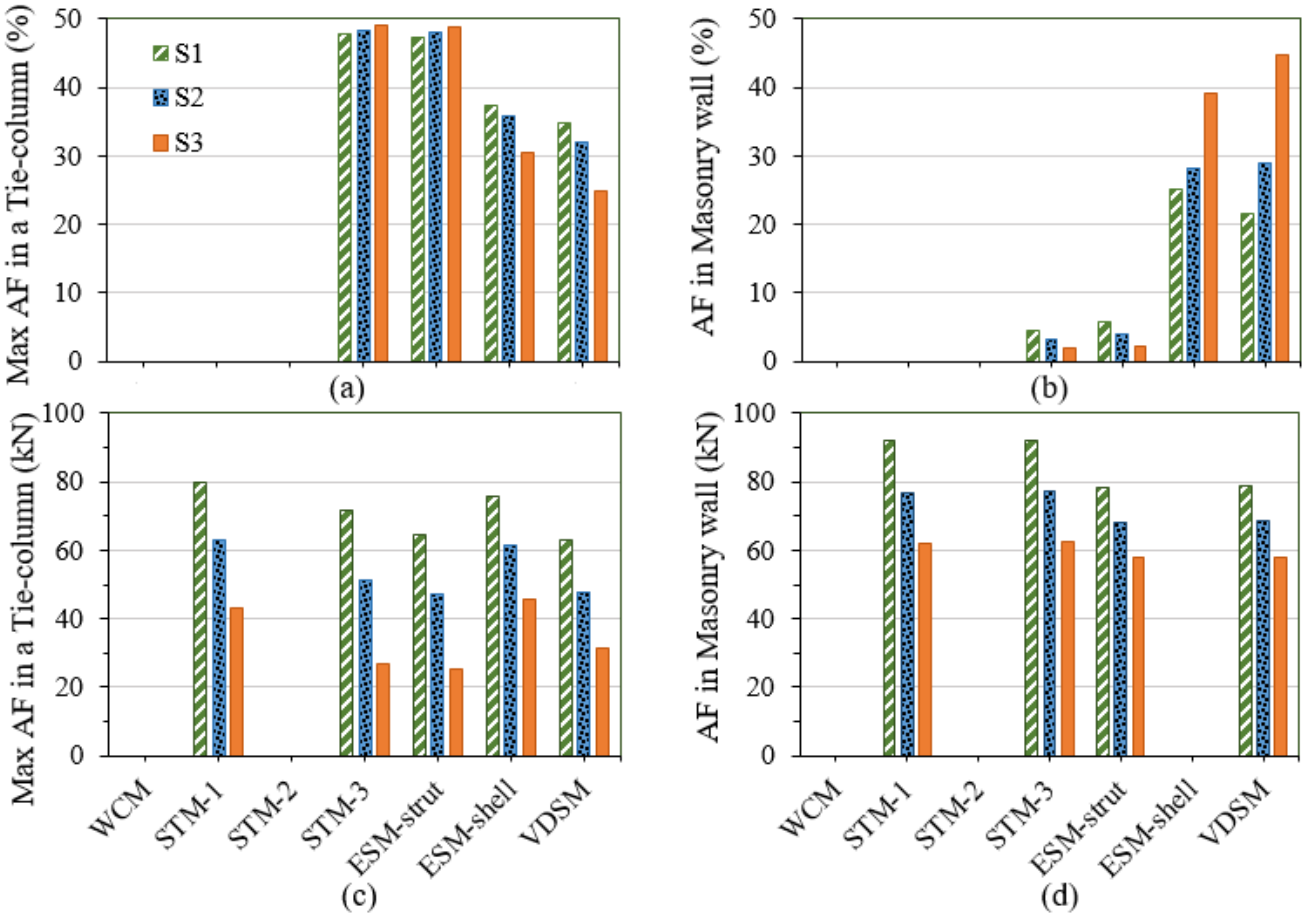

Figure 4

Axial forces in a tie-column and masonry wall obtained from different modeling strategies for CM wall specimens S1, S2, and S3 under (a) and (b) gravity load analysis; (c) and (d) lateral load analysis.

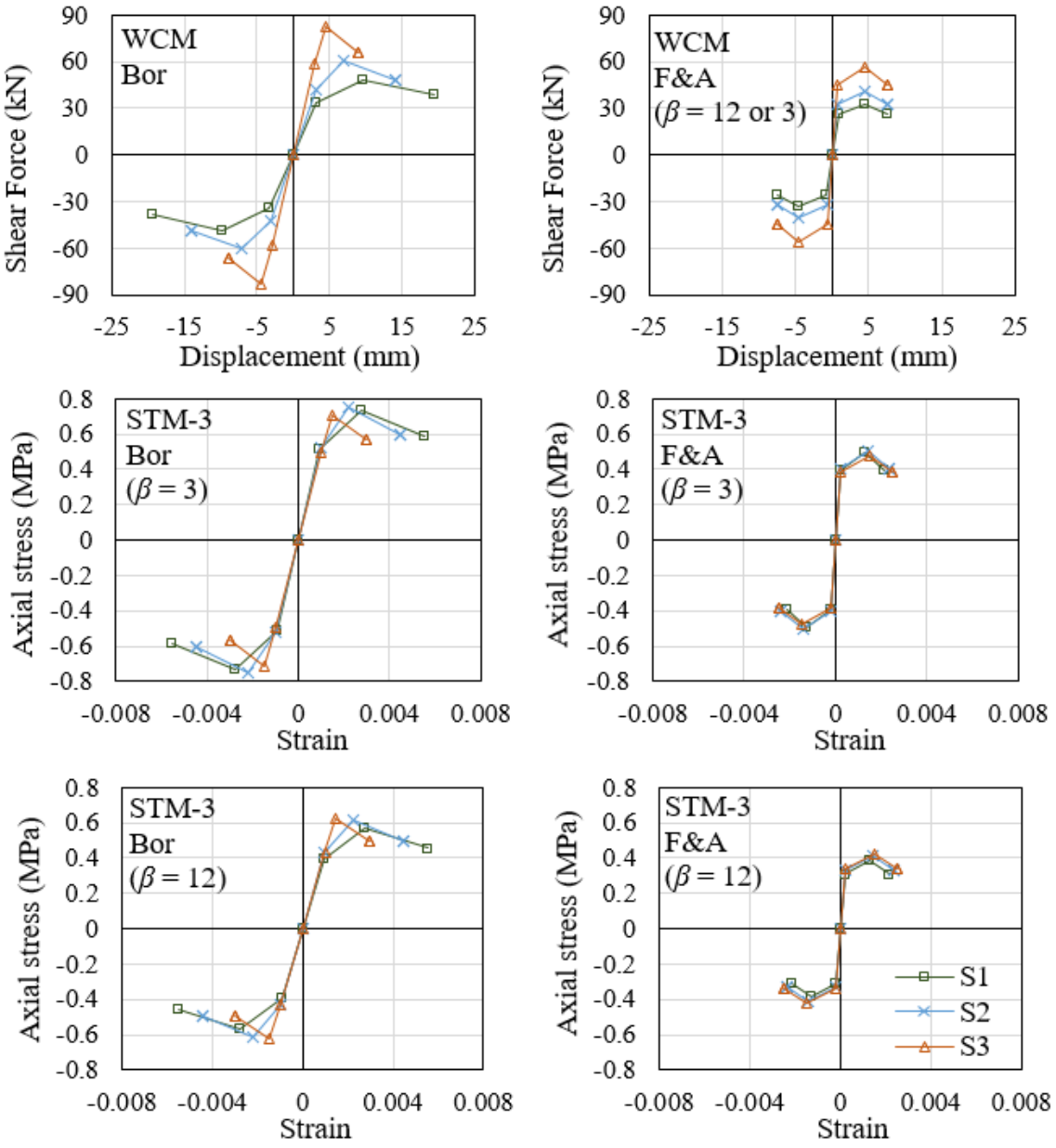

Figure 5

Hinge definitions in WCM and STM-3 for CM walls S1, S2, and S3.

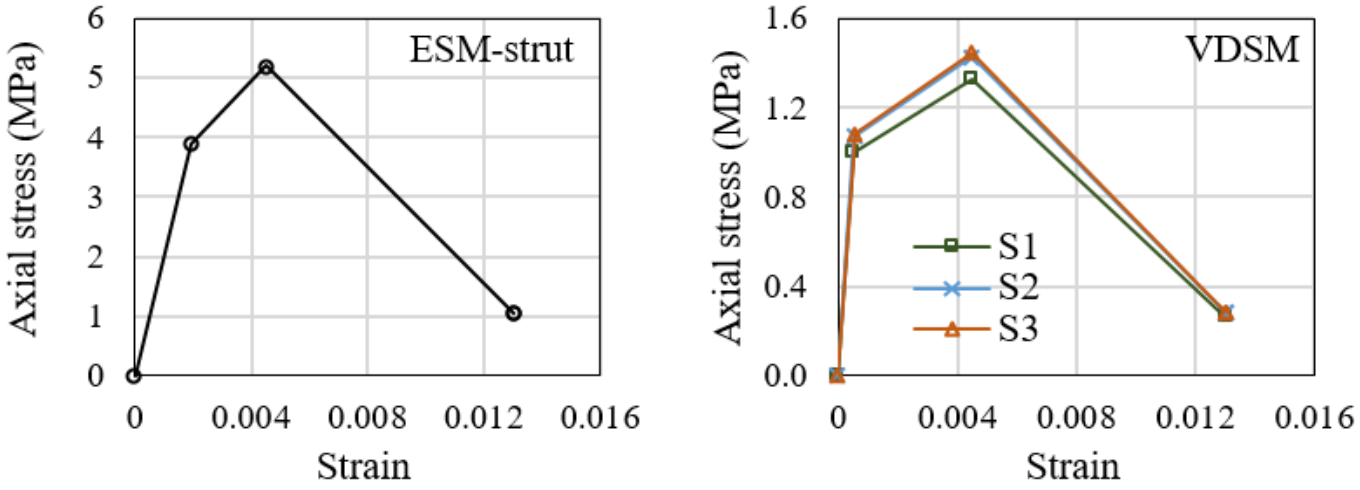

Figure 6

Masonry hinge definitions for CM walls S1, S2, and S3 used in ESM-strut and VDSM.

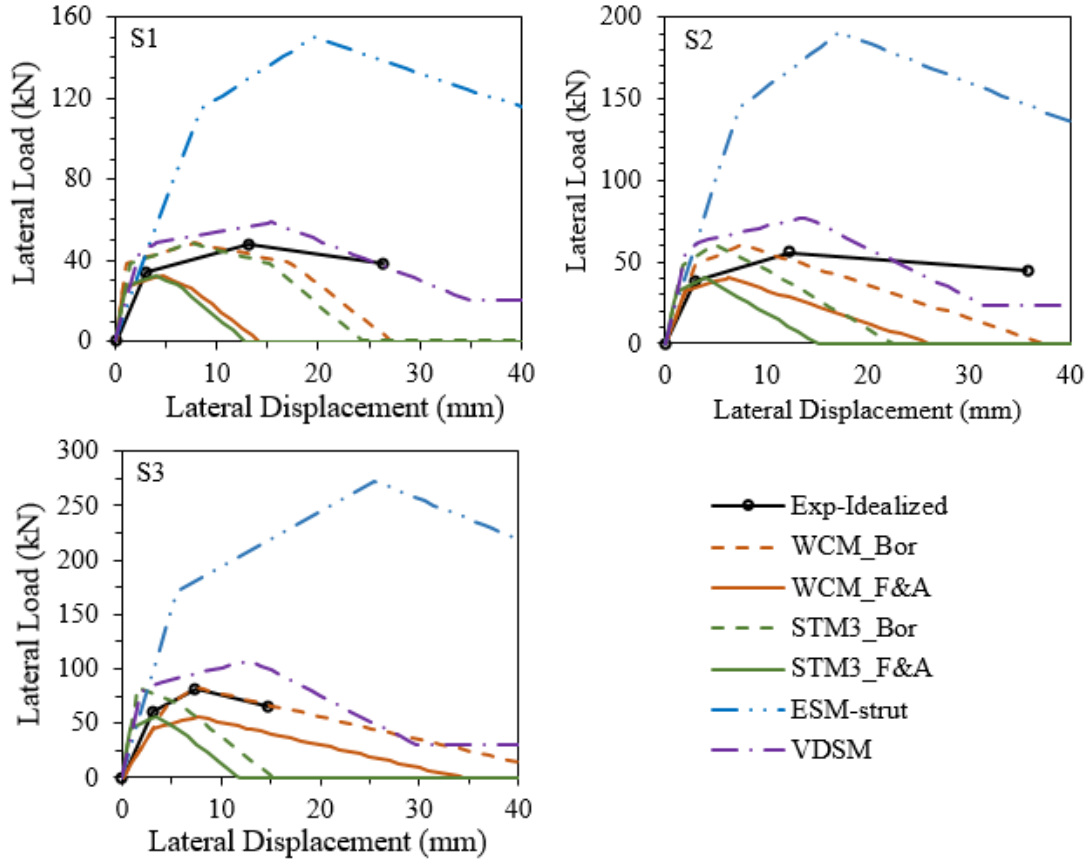

Figure 7

Comparison of experimental results with pushover analysis results for CM walls.

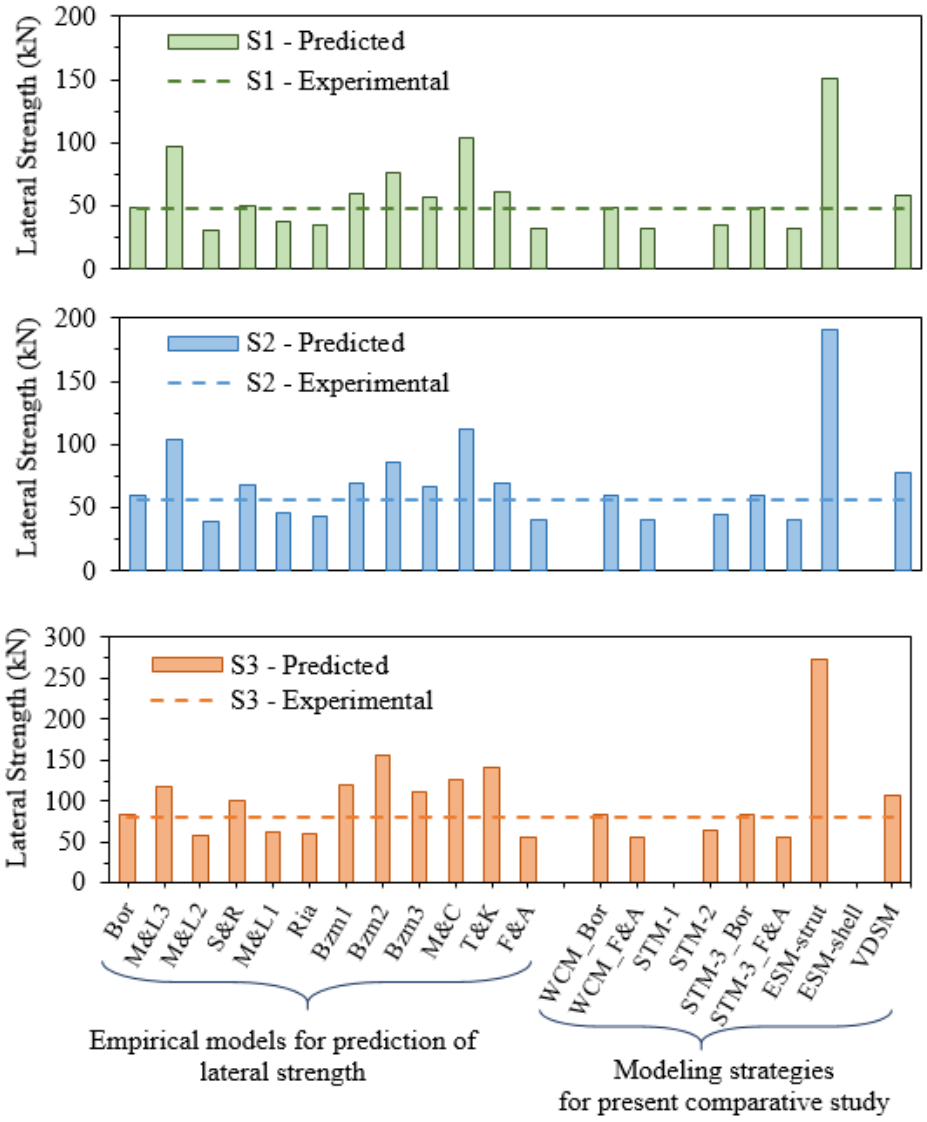

Figure 8

Comparison of lateral strength of CM walls obtained from the tests with that estimated using different modeling strategies and empirical equations.

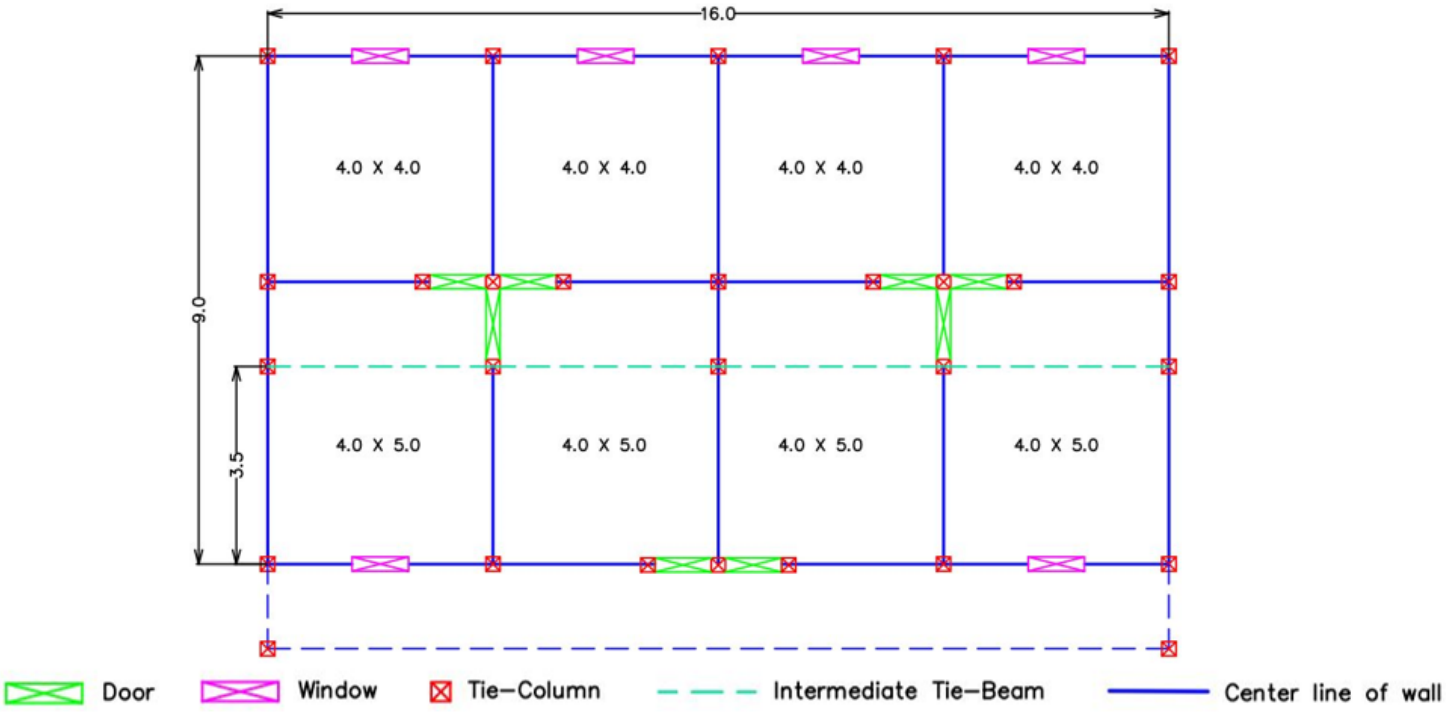

Figure 9

Floor plan of the considered case study building (All dimensions in m).

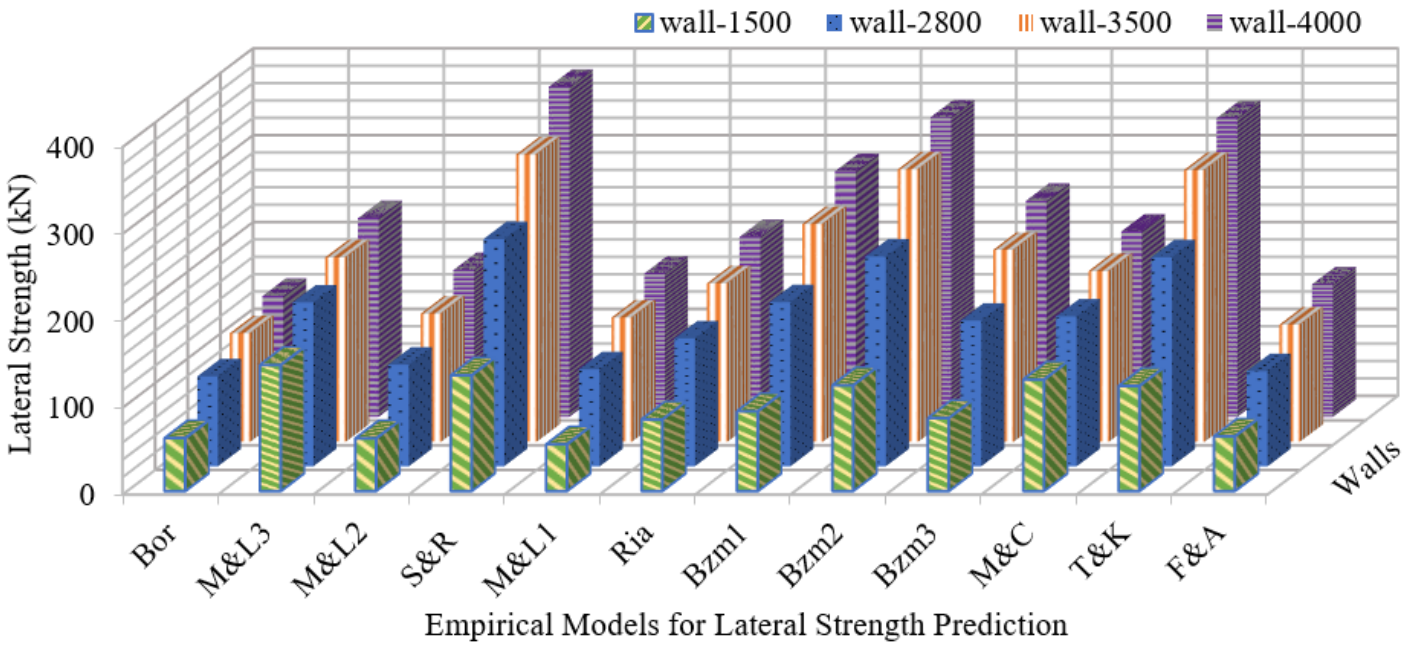

Figure 10

Variation of predicted lateral strength of the CM walls of the case study building using different empirical models.

Figure 11

Hinge definitions for the CM walls of the case study building in different modeling strategies.

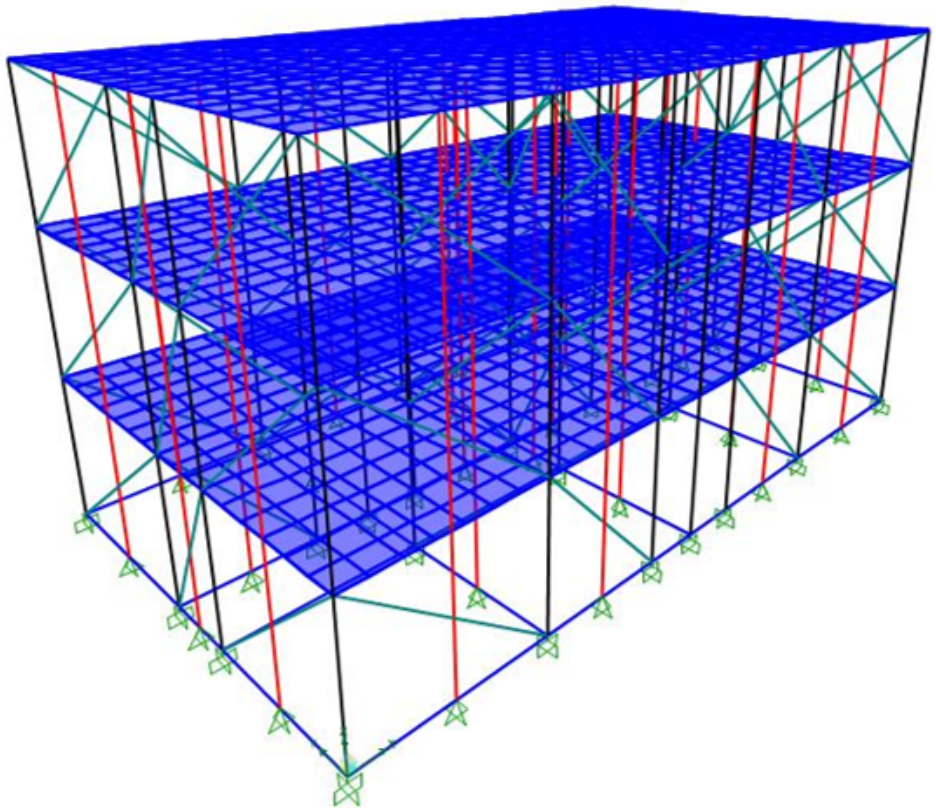

Figure 12

V-D strut model (VDSM) for the case study CM building.

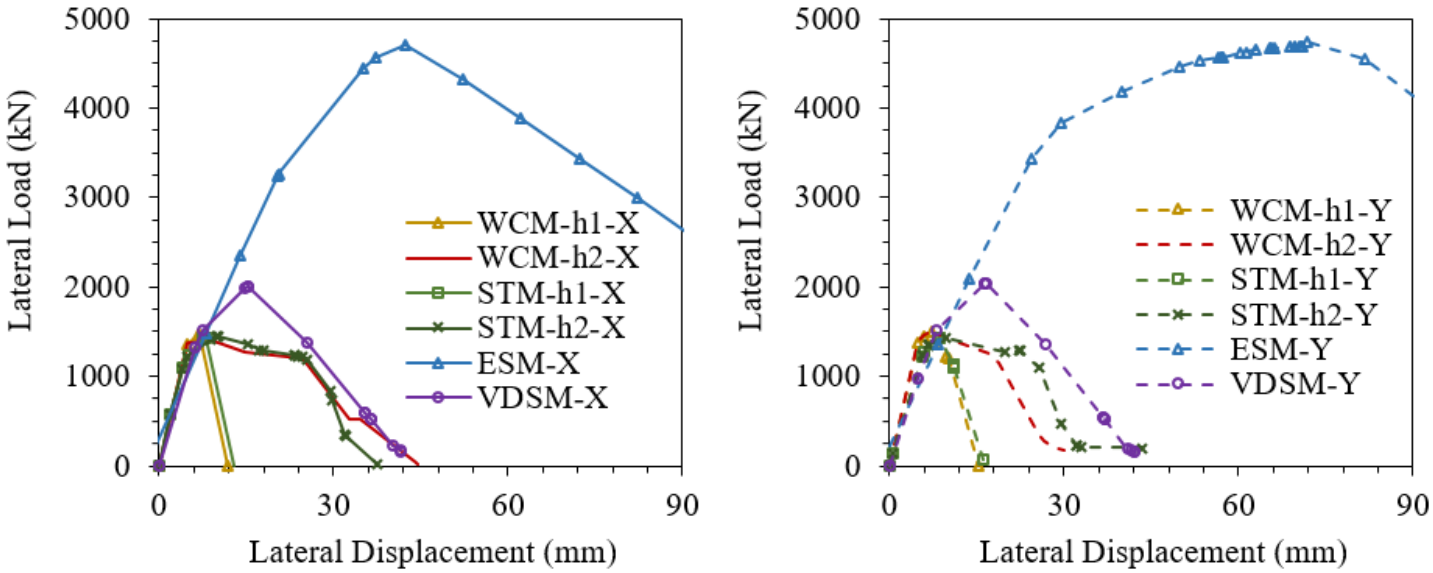

Figure 13

Lateral load response of the case study building using different modeling strategies.